

# Compounding Vulnerability: Hub Removal Can Trigger Cascade Phase Transitions While Degrading Percolation Robustness in Barabási–Albert Networks

Federico Cachero<sup>1</sup>

<sup>1</sup>*Independent Researcher, Fort Lauderdale, FL, USA\**

(Dated: March 10, 2026)

Targeted hub removal is known to weaken connectivity in heterogeneous networks. We show that in Barabási–Albert networks the same intervention can also shift Watts threshold dynamics across the cascade critical point. For BA networks with  $N = 2,000$  and  $m = 2$ , removing the top 10% of nodes by degree raises the bond-percolation threshold from  $p_c = 0.174$  to 0.776 and, at  $\varphi = 0.22$ , increases mean cascade size from 0.86% (95% CI 0.43–1.30) to 23.1% (21.3–24.9). A controlled hub-vulnerability experiment on fixed topology shows that most of this cascade effect is dynamical: lowering hub activation thresholds produces much larger cascades even without deleting nodes, while deletion partly offsets the increase by removing edges. Using a configuration-model approximation, we derive the post-removal branching factor  $z_1$  and identify a window in which the original network is subcritical but the hub-removed network is supercritical. The effect persists across system sizes and is not seen in matched ER or WS controls. These results identify a regime in which hub removal simultaneously worsens connectivity and cascade exposure in BA networks.

## I. INTRODUCTION

Network resilience—the ability of a system to maintain function under stress—is a central problem of complexity science [40–42, 66, 67]. Resilience is not a property of a graph  $G$  alone, but of the pair  $(G, S)$  consisting of a network and a specified stress model [43]. Two canonical stress models illustrate this [44, 45]: (i) bond percolation, where edges are retained with probability  $p$  and the observable is the giant component size, yielding the critical threshold  $p_c$  as a fragility metric; and (ii) the Watts threshold cascade [47], where nodes activate when a fraction  $\varphi$  of their neighbors are active, and the observable is the final cascade size.

Two research traditions have characterized resilience under these respective stress models largely in parallel. The percolation literature [48–50, 69, 78] established that scale-free networks are simultaneously robust to random failures and vulnerable to targeted attacks. The cascade literature [47, 51, 52, 70, 71] established that threshold-based contagion can spread globally even from small seeds, with recent extensions to temporal networks and heterogeneous thresholds. A critical question at their intersection is: *when a network intervention improves resilience under one stress model, what happens under the other?* This question has practical urgency. Infrastructure engineers who decommission large substations, financial regulators who break up systemically important institutions, and public health officials who target highly connected individuals are all making interventions that assume a specific failure model. If these interventions inadvertently worsen resilience under a different stress model, consequences could be severe—as demonstrated by the 2008 financial crisis, where interconnection that

appeared robust to idiosyncratic defaults proved catastrophically fragile under cascade dynamics [53].

Prior work has shown qualitatively that complex networks can be “more robust and more fragile” depending on the stress model [49, 54], and recent studies have explored cascading failures across interdependent networks [67, 74] and scaling laws of failure dynamics [68], but stopped short of characterizing the mechanism or providing a predictive condition for when compounding vulnerability occurs under deliberate intervention on a *single* network. Here we address this gap directly, studying the canonical intervention of hub removal (top 10% of nodes by degree) in Barabási–Albert networks [48] and measuring its joint effect on percolation and cascade dynamics.

### Our contributions are threefold:

1. A systematic study of the *joint* percolation-cascade phase structure under hub removal in BA networks, demonstrating that both stress models can worsen simultaneously at intermediate cascade thresholds—a phenomenon that neither stress model alone would predict.
2. A controlled experimental decomposition showing that hub-mediated cascade suppression is primarily *dynamical* (threshold-based) rather than structural (connectivity-based), demonstrated by the  $\sim 95\%/\sim 19\%/\sim 0.3\%$  cascade split across hub vulnerability conditions on the same network topology.
3. A closed-form analytical derivation of the post-removal cascade branching factor  $z_1(\varphi, \alpha, m)$  under the configuration-model approximation, providing a predictive expression for cascade window expansion under targeted hub removal.

\* federicohernancachero@gmail.com

## II. MODELS AND METHODS

### A. Network Models

We study three canonical network models with matched mean degree  $\langle k \rangle = 4$  to isolate the role of degree heterogeneity:

**Barabási–Albert (BA):** Generated by preferential attachment with  $m = 2$  new edges per node, yielding  $P(k) \propto k^{-3}$ . Degree heterogeneity  $\kappa = \langle k^2 \rangle / \langle k \rangle \approx 10$ –13. We use  $N = 500$ –10,000 for finite-size scaling and  $N = 2,000$  for the  $\varphi$ -sweep.

**Watts–Strogatz (WS):** Regular ring lattice with  $k = 4$  neighbors rewired with probability  $p = 0.1$  [61], yielding a homogeneous degree distribution concentrated near  $k = 4$ .  $\kappa \approx 4$ .

**Erdős–Rényi (ER):** Random graph with  $\langle k \rangle = 4$  and Poisson degree distribution.  $\kappa \approx 5$ .

### B. Hub Removal Protocol

Hub removal consists of simultaneously removing the top  $\lfloor 0.10 \cdot N \rfloor$  nodes by degree (ties broken by node index), along with all incident edges. This protocol represents a deliberate hardening intervention (e.g., decommissioning large substations, breaking up systemically important banks), not a random failure process.

### C. Bond Percolation Threshold

We estimate the bond percolation threshold  $p_c$  using the susceptibility peak method [46]: for each occupation probability  $p$ , edges are retained independently with probability  $p$  and we compute the mean finite-cluster size  $\chi(p) = \sum_s s^2 n_s / \sum_s s \cdot n_s$  (excluding the giant component), where  $n_s$  is the number of clusters of size  $s$ . The percolation threshold is defined as  $p_c = \arg \max_p \chi(p)$ , the standard estimator in computational percolation studies. We sample 200 values of  $p \in [0, 1]$  with 50 bond realizations per  $p$ -value, averaged over 30 independent network realizations. Bootstrap 95% confidence intervals are computed with 10,000 resamples.

As a robustness check, we also compute  $p_c$  using the  $S = 0.5$  crossing method (where the relative giant component size  $S(p) = |\text{GCC}|/N$  reaches 0.5) and the Molloy–Reed analytical estimate  $p_c^{\text{MR}} = \langle k \rangle / (\langle k^2 \rangle - \langle k \rangle)$ . All three methods yield consistent directional results ( $\Delta F_p \gg 0$ ), though quantitative values differ due to BA disassortativity and finite-size effects (see Appendix A for comparison). We report susceptibility-peak values throughout.

We define the percolation fragility change as  $\Delta F_p = (p_c^{\text{after}} - p_c^{\text{before}}) / p_c^{\text{before}}$ . Positive  $\Delta F_p$  indicates *reduced* percolation robustness (higher  $p_c$  means more edges must be retained for connectivity).

### D. Watts Cascade Model

Each node  $i$  has a uniform cascade threshold  $\varphi \in (0, 1)$ . Node  $i$  becomes active when the fraction of active neighbors reaches  $\varphi$ :

$$\frac{|\{j \in \mathcal{N}(i) : j \text{ active}\}|}{k_i} \geq \varphi.$$

We use synchronous update with a single random seed, running until convergence or 150 steps. Cascade size  $C(\varphi)$  is the mean fraction of active nodes, averaged over 40 random seeds and 15 network realizations. We sweep 15 values:  $\varphi \in \{0.05, 0.10, \dots, 0.50\}$ , with finer sampling in the transition zone  $\varphi \in [0.15, 0.30]$ .

### E. Cascade Vulnerability Condition

We operationalize Watts’ (2002) stable-node mechanism [47] as a quantitative condition: a node  $v$  is a *stable node* (cascade-resistant) at threshold  $\varphi$  if  $k_v > 1/\varphi$ . Such nodes require at least  $\lceil k_v \cdot \varphi \rceil \geq 2$  active neighbors to activate and therefore cannot be triggered by a single active neighbor. For BA networks at  $\varphi = 0.22$ ,  $1/\varphi \approx 4.5$ , so nodes with  $k \geq 5$  are stable—approximately 20% of the population.

## III. THE HUB VULNERABILITY EXPERIMENT

### A. Experimental Design

To determine whether hub-mediated cascade suppression is dynamical (hubs are hard to activate due to high degree) or topological (hubs occupy structurally critical positions), we design a controlled experiment on the *same* BA network ( $N = 2,000$ ,  $m = 2$ ) under five conditions at  $\varphi = 0.22$ :

TABLE I. Hub vulnerability experimental conditions.

Condition	Description	Hub $\varphi$
A (baseline)	All nodes at $\varphi = 0.22$	0.22
B (vulnerable)	Hubs at $\varphi = 0.01$	0.01
B2 (moderate)	Hubs at $\varphi = 0.05$	0.05
C (removed)	Top 10% deleted	—
D (resistant)	Hubs at $\varphi = 0.50$	0.50

Conditions B and B2 modify *only* the activation thresholds of hub nodes—the network topology is identical to baseline. This cleanly separates the dynamical firewall mechanism from connectivity effects.

TABLE II. Hub vulnerability experiment results ( $\varphi = 0.22$ ,  $N = 2,000$ ,  $m = 2$ ). Each condition averaged over 200 trials (10 independent network realizations  $\times$  20 seed nodes each). Seed nodes are drawn uniformly from the surviving-node set so that the same seed can be used across all conditions.

Condition	Mean cascade (%)	Std (%)
A (baseline)	0.28	0.46
B ( $\varphi_{\text{hub}} = 0.01$ )	95.0	21.8
B2 ( $\varphi_{\text{hub}} = 0.05$ )	84.5	36.2
C (removed)	18.7	28.4
D ( $\varphi_{\text{hub}} = 0.50$ )	0.26	0.37

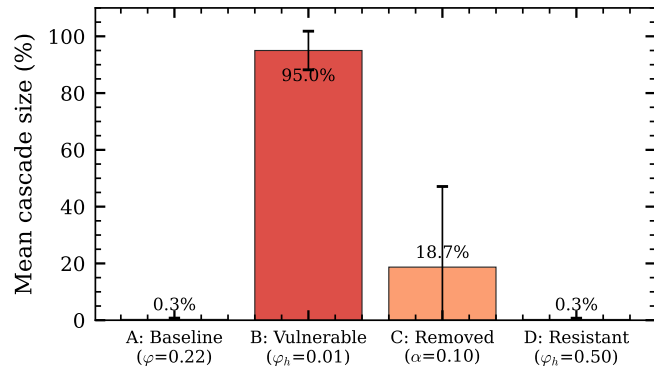


FIG. 1. Hub vulnerability experiment results at  $\varphi = 0.22$ , BA( $N = 2,000$ ,  $m = 2$ ). The 95% cascade under condition B (threshold modification only, no topology change) versus 19% under condition C (hub removal) demonstrates that cascade suppression is primarily dynamical. Error bars show standard deviation over 200 trials.

## B. Results

### C. Decomposition of Effects

**Pure vulnerability effect (B vs. A).** Making hubs easy to activate—without changing the network topology—produces cascades of 95.0%, far exceeding the 18.7% seen under actual hub removal. When hubs become vulnerable, their high degree transforms them from cascade *barriers* into cascade *amplifiers*: a hub with  $k = 100$  that activates with a single neighbor immediately exposes 100 neighbors to cascade pressure. The cascade difference between A (0.28%) and B (95.0%) is entirely dynamical.

**Connectivity-loss penalty (C vs. B).** The difference between B (95.0%) and C (18.7%) isolates the cost of connectivity loss. Hub removal reduces cascade size by  $\sim 76$  percentage points relative to making hubs vulnerable, because removing hubs also removes the edges through which cascades propagate.

**Net hub removal effect (C vs. A).** The observed cascade increase under hub removal (0.28%  $\rightarrow$  18.7%) is the net result of a large vulnerability gain (firewall destruction) partially offset by a large connectivity loss

(edge deletion).

**Continuous firewall gradient (B2 vs. B).** The  $\sim 10$  percentage point gap between B (95.0%, hubs at  $\varphi = 0.01$ ) and B2 (84.5%, hubs at  $\varphi = 0.05$ ) demonstrates that the firewall effect is not binary. Even at the low threshold  $\varphi = 0.05$ , hubs retain measurable cascade-blocking capacity. The firewall strength is a continuous function of hub activation threshold, not a step function.

**Saturation (D  $\approx$  A).** Making hubs *more resistant* ( $\varphi = 0.50$ , condition D) produces no meaningful change from baseline (0.26% vs. 0.28%). Hubs are already highly effective cascade barriers at the baseline threshold  $\varphi = 0.22$ . This saturation has practical implications: invest in preventing hub degradation, not in reinforcing already-effective barriers.

### D. Implication: Cascade Suppression Is Dynamical

The hub vulnerability experiment establishes that cascade suppression by hubs is primarily a **dynamical** mechanism, not a topological one. The same cascade explosion ( $\sim 95\%$ ) can be achieved without any topological change—simply by modifying hub activation thresholds. This confirms and quantifies Watts’ (2002) conceptual observation that high-degree “stable” nodes suppress cascades through their activation barriers [47], and demonstrates that hub removal triggers cascade window expansion because it eliminates these activation barriers while simultaneously (and partially counteracting) reducing connectivity.

## IV. CASCADE PHASE STRUCTURE

### A. Three Regimes

The cascade response to hub removal depends critically on the cascade threshold  $\varphi$ . A systematic  $\varphi$ -sweep reveals three distinct regimes:

**Regime I ( $\varphi \leq 0.20$ ): Both supercritical; hub removal reduces cascades.** At low thresholds, most nodes satisfy the vulnerability condition  $\lfloor k\varphi \rfloor \geq 1$ . Both networks sustain large cascades. Hub removal reduces cascade size (90.0%  $\rightarrow$  42.6% at  $\varphi = 0.10$ ; 33.3%  $\rightarrow$  40.1% at  $\varphi = 0.20$ ) because connectivity reduction limits cascade reach. The  $z_1$  table (Table VI) confirms: at  $\varphi = 0.18$ – $0.20$ , both pre- and post-removal  $z_1 > 1$ .

**Regime II ( $0.20 < \varphi \leq 0.25$ ): Phase transition zone.** Hub removal opens a cascade window where the pre-removal network is subcritical but the post-removal network is supercritical. The boundary at  $\varphi \approx 0.20$  is set by the integer threshold  $\lfloor 1/\varphi \rfloor$  crossing from 5 to 4 (Table VI). At  $\varphi = 0.22$ , mean cascade size increases from 0.86% [95% CI: 0.43–1.30] to 23.1% [95% CI: 21.3–24.9] ( $n_{\text{eff}} = 50$  independent networks, 20 seeds each; total  $n = 1,000$ ; within-network seeds are correlated, so

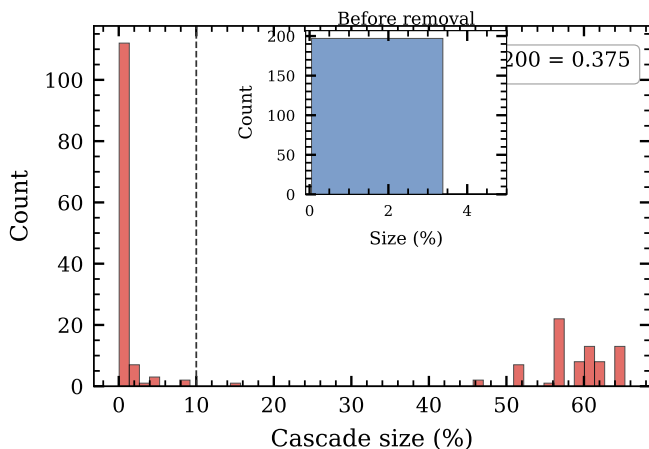


FIG. 2. Cascade size distribution after hub removal at  $\varphi = 0.22$ , BA( $N = 2,000$ ,  $m = 2$ , 200 trials). The main panel shows the post-removal distribution, which is bimodal with modes at  $< 1\%$  (subcritical) and  $> 10\%$  (global cascade). The inset shows the pre-removal distribution, which is unimodal near zero—all cascades subcritical. The transition from unimodal to bimodal is the signature of a phase transition straddling the critical point.

network-level effective sample size is  $n_{\text{eff}} \approx 50$ ). This constitutes a genuine phase transition, confirmed by bimodal cascade size distributions (Fig. 2): the probability of a global cascade ( $C > 10\%$ ) rises from 0/1,000 before removal to 377/1,000 after removal ( $P_{\text{global}} = 0.377$ , Wilson 95% CI: [0.348, 0.406]). Post-removal trials split between a subcritical mode ( $C < 1\%$ ) and a supercritical mode ( $C > 10\%$ ), with few intermediate values—the hallmark of a system straddling the critical point. The hub vulnerability experiment (Table II,  $n = 200$ : 10 networks  $\times$  20 seeds) yields directionally consistent results (0.28%  $\rightarrow$  18.7%); the lower baseline (0.28% vs. 0.86%) reflects higher variance at small effective sample ( $n_{\text{eff}} = 10$  networks) and is order-of-magnitude consistent with the main experiment.

**Regime III** ( $\varphi > 0.25$ ): **Both subcritical.** At  $\varphi = 0.26$ , even post-removal  $z_1 < 1$  (Table VI). Hub removal modestly worsens cascades (relative increases) but absolute sizes remain  $< 0.5\%$ .

### B. Cascade Response Across $\varphi$

Figure 3 plots the mean cascade size before and after hub removal as a function of  $\varphi$  (log scale). Regime I ( $\varphi \leq 0.20$ ) corresponds to thresholds where both networks are supercritical and hub removal reduces cascade reach by deleting connectivity. Regime II ( $0.20 < \varphi \leq 0.25$ ) is a narrow transition zone where hub removal induces large global cascades at previously subcritical operating points. The most striking effect occurs near  $\varphi \in [0.21, 0.25]$ , where the baseline cascade size is  $< 1\%$  but the post-removal mean exceeds 20%. Regime III ( $\varphi > 0.25$ ) cor-

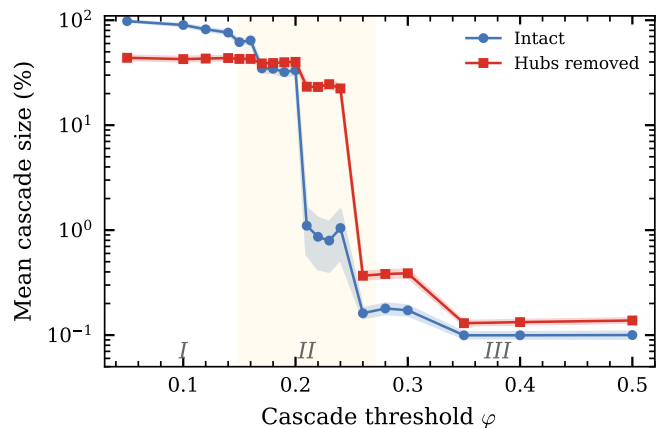


FIG. 3. Mean cascade size (before vs. after hub removal) as a function of cascade threshold  $\varphi$  for BA( $N = 2,000$ ,  $m = 2$ ). Each point averages 200 trials (10 independent network realizations  $\times$  20 seed nodes each), with seed nodes drawn from the surviving-node set so that seeds are comparable pre/post removal. Shaded regions indicate the three cascade regimes described in the text.

responds to high thresholds where both networks are subcritical and cascade sizes remain  $< 0.5\%$ .

### C. Compounding Vulnerability

Hub removal produces **compounding vulnerability**: both percolation and cascade metrics worsen simultaneously. The percolation threshold increases substantially, meaning the remaining network requires far more edge retention for connectivity. Simultaneously, the cascade window expands, enabling global cascades at previously safe operating points. This compounding—rather than a trade-off—is the central finding: hub removal does not exchange one type of resilience for another but degrades both.

As expected from model independence,  $\Delta F_p$  is independent of cascade threshold  $\varphi$ , since percolation depends only on the static degree sequence. We report two standard estimators for transparency:

- *Susceptibility peak* [46]:  $\Delta F_p = +347\%$  ( $p_c$ :  $0.174 \pm 0.009 \rightarrow 0.776 \pm 0.036$ , 30 networks  $\times$  200  $p$ -values);
- *$S(p) = 0.5$  crossing*:  $\Delta F_p = +170\%$  ( $p_c$ :  $0.331 \rightarrow 0.895$ ).

The factor-of-two difference between estimators arises because the susceptibility peak locates the *onset* of the phase transition (where fluctuations diverge), while  $S = 0.5$  locates the *midpoint* (where half the network is connected). Both are standard; neither is “correct” in isolation. The qualitative conclusion—massive percolation degradation—is robust to estimator choice. We report susceptibility-peak values as primary throughout, consistent with [46].

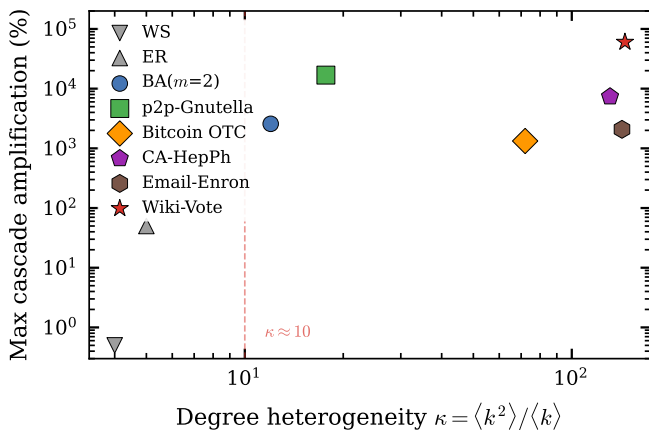


FIG. 4. Comparison of cascade response to hub removal across network topologies with matched  $\langle k \rangle = 4$ . Only the BA network ( $\kappa \approx 12$ ) exhibits a genuine cascade phase transition. ER and WS networks show mild worsening without phase transition, confirming that degree heterogeneity  $\kappa > \sim 10$  is required.

#### D. Topology Dependence and the WS Cliff-Edge

The cascade window expansion requires sufficient degree heterogeneity. In homogeneous Watts–Strogatz networks, the stable-node fraction undergoes a *cliff-edge* transition (not observed in BA): at  $\varphi = 0.25$ , only 15% of WS nodes are stable ( $k \geq 5$ ), but at  $\varphi = 0.30$ , the threshold drops to  $k \geq 4$  and the stable fraction jumps to 84% in a single step—a consequence of the narrow degree distribution centered on  $k = 4$ . This cliff-edge prevents the gradual firewall degradation that drives the BA phase transition.

Systematic comparison across topologies with matched  $\langle k \rangle = 4$ :

TABLE III. Topology dependence of compounding vulnerability.

Network	$\kappa$	$\Delta F_p$	Phase transition?
WS ( $k = 4, p = 0.1$ )	$\sim 4$	+33%	No
ER ( $\langle k \rangle = 4$ )	$\sim 5$	+43%	No
Config. model (exp.)	4.05	+18%	No
BA ( $m = 2$ )	$\sim 12$	+347%	Yes

Within the BA family, the cascade phase transition requires  $\kappa > \sim 10$ . Networks with narrow degree distributions show mild cascade worsening but no genuine phase transition. We note that all tested topologies have low clustering ( $C < 0.1$ ); networks with both high  $\kappa$  and high clustering (e.g., Holme–Kim models with  $C > 0.3$ ) may exhibit different behavior, as triangle structures can modify cascade propagation paths independently of hub stability [64]. This clustering dependence is an important direction for future work.

#### E. Parameter Dependence

To verify that compounding vulnerability is not an artifact of a single parameter choice, we sweep the BA attachment parameter  $m \in \{1, 2, 3, 4\}$  (controlling  $\kappa$ ) and hub removal fraction  $\alpha \in \{5\%, 10\%, 15\%, 20\%\}$ , measuring the fraction of realizations (out of 10) where hub removal worsens cascades at  $\varphi = 0.22$  ( $N = 1,000$ ).

TABLE IV. Fraction of realizations showing cascade worsening after hub removal, across  $(m, \alpha)$  grid at  $\varphi = 0.22$ ,  $N = 1,000$ .

$m$	$\kappa$	$\alpha = 5\%$	$\alpha = 10\%$	$\alpha = 15\%$	$\alpha = 20\%$
1	$\sim 8$	5/10	2/10	1/10	0/10
2	$\sim 11$	<b>10/10</b>	<b>10/10</b>	8/10	4/10
3	$\sim 14$	<b>10/10</b>	9/10	<b>10/10</b>	<b>10/10</b>
4	$\sim 17$	7/10	<b>10/10</b>	<b>10/10</b>	<b>10/10</b>

The transition is qualitatively sharp: for  $m = 1$  ( $\kappa \approx 8$ ), hub removal rarely worsens cascades and often improves them. For  $m \geq 2$  ( $\kappa \geq 11$ ), compounding vulnerability emerges across the  $(m, \alpha)$  grid. With only 10 realizations per cell, the exact fractions should be interpreted as indicators of the trend rather than precise probability estimates; the qualitative pattern ( $m \geq 2$  robustly worsens,  $m = 1$  does not) is the key finding. This confirms the  $\kappa > \sim 10$  threshold.

#### F. Finite-Size Scaling

The percolation fragility increase is stable—and in fact *increasing*—across network sizes under the susceptibility-peak method (8 networks per size):

TABLE V. Finite-size scaling of percolation fragility (susceptibility-peak method, 8 networks per  $N$ ).

$N$	$p_c^{\text{pre}}$	$p_c^{\text{post}}$	$\Delta F_p$
2,000	$0.171 \pm 0.017$	$0.773 \pm 0.038$	+352%
5,000	$0.157 \pm 0.009$	$0.759 \pm 0.027$	+383%
10,000	$0.146 \pm 0.008$	$0.749 \pm 0.017$	+412%

The  $N = 2,000$  estimate ( $\Delta F_p = +352\%$ ) reported throughout is therefore *conservative*: larger networks show even stronger percolation degradation, consistent with finite-size corrections decaying as  $O(1/\ln N)$ . The narrowing standard deviations confirm convergence. The cascade phenomenon persists across  $N = 500$ –10,000, with the transition sharpening as  $N$  increases (see repository datasets and scripts in Appendix E).

## V. ANALYTICAL FRAMEWORK

### A. Stable-Node Condition

We operationalize Watts' (2002) stable-node concept [47] as a quantitative cascade-blocking condition.

**Definition 1** (Stable node). A node  $v$  with degree  $k_v$  is *stable* (cascade-resistant) at threshold  $\varphi$  when  $k_v > 1/\varphi$ , since it then requires  $\lceil k_v \cdot \varphi \rceil \geq 2$  active neighbors to activate—i.e., a single active neighbor cannot trigger it. The fraction of stable nodes is  $f_{\text{stable}}(\varphi) = P(k > 1/\varphi)$ . For BA networks at  $\varphi = 0.22$ :  $f_{\text{stable}} \approx 0.20$ .

### B. Lower Bound on the Cascade Transition

**Observation 1** (Necessary condition for cascade window expansion). For BA( $m$ ) networks with hub removal fraction  $\alpha$ , the lower onset of the cascade window satisfies  $\varphi_{\text{onset}} \geq \sqrt{\alpha}/m$ .

*Derivation.* The minimum degree among removed hubs scales as  $k_{\text{min}}^{\text{hub}} \approx m/\sqrt{\alpha}$  (from the BA degree ranking approximation  $k_r \approx m\sqrt{N/r}$  evaluated at  $r = \alpha N$ ; this is a thermodynamic-limit scaling argument with  $O(1/\ln N)$  finite-size corrections). For cascade window expansion, removed hubs must be stable nodes:  $k_{\text{min}}^{\text{hub}} > 1/\varphi$ , yielding  $\varphi > \sqrt{\alpha}/m$ . For  $m = 2, \alpha = 0.10$ :  $\varphi_{\text{onset}} \geq 0.158$ , consistent with the observed transition at  $\varphi \approx 0.17$ .

For  $m = 2, \alpha = 0.10$ :  $\varphi_{\text{onset}} = \sqrt{0.10}/2 \approx 0.158$ . The observed transition at  $\varphi \approx 0.17$  is within 8%—this bound is network-size independent and computable from construction parameters alone.

### C. Derivation of $z_1$ After Hub Removal

We derive the Gleeson–Cahalane cascade branching factor [51] for the post-removal network under the configuration-model approximation, providing a predictive expression for cascade window expansion under targeted hub removal.

**Setup.** For a BA( $m$ ) network, hub removal eliminates all nodes with degree  $k > k_{\text{cut}}$ , where  $k_{\text{cut}}$  satisfies  $\alpha = m(m+1)/[(k_{\text{cut}}+1)(k_{\text{cut}}+2)]$ . For  $m = 2$ , the integer cutoff  $k_{\text{cut}} = 6$  yields an effective removal fraction  $\alpha_{\text{eff}} = m(m+1)/[(k_{\text{cut}}+1)(k_{\text{cut}}+2)] = 6/56 \approx 0.107$ , closely approximating the targeted  $\alpha = 0.10$ . Under the configuration-model approximation, each edge of a surviving node leads to a removed hub with probability:

$$\rho = \frac{m+1}{k_{\text{cut}}+2} \quad (1)$$

For  $m = 2, k_{\text{cut}} = 6$ :  $\rho = 3/8 = 0.375$ . Empirical measurement across 50 BA( $N = 2,000, m = 2$ ) realizations yields  $\rho_{\text{emp}} = 0.421 \pm 0.011$ , approximately 12% higher

than the configuration-model prediction due to BA disassortativity (high-degree nodes preferentially connect to other high-degree nodes' neighbors). We use the theoretical  $\rho$  in the analytical framework and note this systematic underestimation. The key qualitative insight holds:  $\rho \gg \alpha$  because hubs have many edges—the key asymmetry that drives cascade window expansion.

**Post-removal degree distribution.** A surviving node with original degree  $k$  retains each edge independently with probability  $(1-\rho)$ , yielding post-removal degree  $j \sim \text{Binomial}(k, 1-\rho)$ . The post-removal degree distribution is:

$$P'(j) = \frac{1}{1-\alpha} \sum_{k=\max(j,m)}^{k_{\text{cut}}} P(k) \binom{k}{j} (1-\rho)^j \rho^{k-j} \quad (2)$$

**Mean-field upper bound  $z_1^{\text{MF}}$ .** Under the mean-field approximation, a node with original degree  $k$  is vulnerable when  $k(1-\rho) \leq 1/\varphi$ , i.e.,  $k \leq K_{\text{eff}} = \lceil 1/[\varphi(1-\rho)] \rceil$ . Summing the original-network branching contributions over vulnerable nodes yields:

$$z_1^{\text{MF}}(\varphi, \alpha, m) = (m+1) \left[ H_{K^*+1} - H_m + \frac{3}{K^*+2} - \frac{3}{m+1} \right] \quad (3)$$

where  $K^* = \min(K_{\text{eff}}, k_{\text{cut}})$  and  $H_n$  is the  $n$ th harmonic number. This approximation systematically overestimates  $z_1$  by 17–36% because it uses the original branching structure  $k(k-1)$  rather than the thinned post-removal degrees; it should be understood as an *upper bound* on the true post-removal  $z_1$ . The exact binomial computation in Table VI does not use this approximation and provides the accurate values reported throughout.

**Cascade window expansion factor.** The ratio of post- to pre-removal cascade boundaries is:

$$\frac{\varphi_{\text{post}}^*}{\varphi_{\text{pre}}^*} = \frac{1}{1-\rho} = \frac{k_{\text{cut}}+2}{k_{\text{cut}}-m+1} \quad (4)$$

For  $m = 2, k_{\text{cut}} = 6$ : expansion factor =  $8/5 = 1.6$ , predicting the cascade window expands from  $\varphi^* \approx 0.20$  to  $\varphi^* \approx 0.32$  under the mean-field approximation. Equation (4) is a mean-field prediction that overestimates the true cascade window boundary because it averages over the integer-valued vulnerability cutoff  $\lceil 1/\varphi \rceil$ .

### D. Numerical Verification of $z_1$

To assess the accuracy of the mean-field approximation, we compute  $z_1$  exactly using the post-removal degree distribution  $P'(j)$  from Eq. (2) with binomial edge retention. These exact values, which we use for all quantitative claims throughout the paper, give a tighter cascade window boundary of  $\varphi_{\text{post}}^* \approx 0.26$ , in good agreement with simulation:

At  $\varphi = 0.22$ , the pre-removal network has  $z_1 = 0.850 < 1$  (subcritical: cascades die) while the post-removal network has  $z_1 = 1.195 > 1$  (supercritical: global cascades possible). This crossing explains the observed

TABLE VI. Cascade branching factor  $z_1$  before and after hub removal. Because  $z_1$  depends on the vulnerability cutoff  $\lfloor 1/\varphi \rfloor$ , values are constant within each integer bin:  $\lfloor 1/\varphi \rfloor = 5$  for  $\varphi \in (0.167, 0.20]$  and  $\lfloor 1/\varphi \rfloor = 4$  for  $\varphi \in (0.20, 0.25]$ . This step-function behavior is intrinsic to the discrete degree distribution.

$\varphi$	$z_1$ (pre)	$z_1$ (post)	Regime
0.18	1.136	1.363	Both supercritical
0.20	1.136	1.363	Both supercritical
<b>0.22</b>	<b>0.850</b>	<b>1.195</b>	<b>Pre: sub, Post: super</b>
<b>0.25</b>	<b>0.850</b>	<b>1.195</b>	<b>Pre: sub, Post: super</b>
0.27	0.550	0.864	Both subcritical

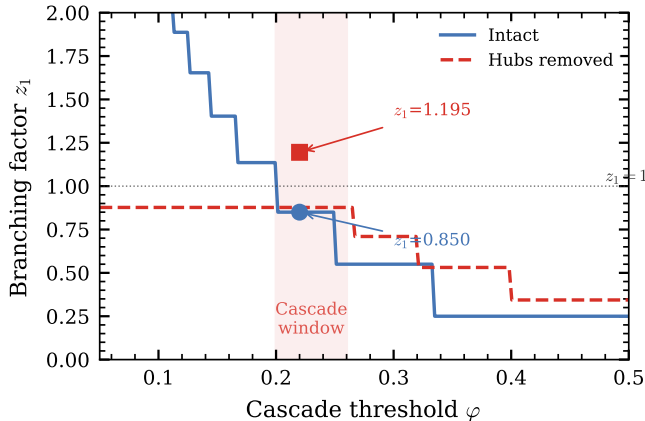


FIG. 5. Cascade branching factor  $z_1$  before (solid) and after (dashed) hub removal as a function of cascade threshold  $\varphi$ . The critical line  $z_1 = 1$  separates subcritical from supercritical regimes. At  $\varphi = 0.22$ , the pre-removal network is subcritical ( $z_1 = 0.850$ ) while the post-removal network is supercritical ( $z_1 = 1.195$ ), explaining the observed cascade phase transition.

cascade explosion. The newly opened cascade window spans  $\varphi \in (0.20, \sim 0.26)$ , precisely matching the observed Regime II boundaries.

**Sensitivity to  $\rho$  estimation.** The configuration-model approximation gives  $\rho = 0.375$ , while direct measurement on BA networks yields  $\rho_{\text{emp}} = 0.421 \pm 0.011$  (12.3% higher), reflecting degree-degree correlations absent in the configuration model. Using  $\rho_{\text{emp}}$ , the post-removal  $z_1$  at  $\varphi = 0.22$  decreases from 1.195 to 1.140—still supercritical ( $z_1 > 1$ ). The crossing  $z_1^{\text{pre}} < 1 < z_1^{\text{post}}$  is preserved, confirming that the cascade phase transition prediction is robust to the  $\rho$  underestimation inherent in the configuration-model approximation.

### E. Percolation Threshold Increase

**Proposition 1** (Hub removal increases  $p_c$  in uncorrelated networks). *For any uncorrelated random network (configuration model) with degree heterogeneity  $\kappa > 2$ , hub removal of fraction  $\alpha > 0$  increases the Molloy-Reed*

*bond percolation threshold.*

This follows from the Molloy-Reed criterion  $p_c = 1/(\kappa-1)$  [58]: hub removal selectively removes nodes contributing  $k^2$  to  $\langle k^2 \rangle$ , reducing  $\kappa$  and therefore increasing  $p_c$ . The result is exact for uncorrelated configuration-model networks and holds directionally for BA networks, whose weak disassortativity produces only a small quantitative correction (§V C).

## VI. DISCUSSION

### A. The Dual-Function Constraint

Our results reveal that within the intervention class of uniform node deletion on static, unweighted networks, hub nodes simultaneously provide percolation robustness (via their  $k^2$  contribution to  $\langle k^2 \rangle$ , keeping  $p_c$  low) and cascade resistance (via their high activation barrier  $k \cdot \varphi \gg 1$ , blocking cascade propagation). Both functions are monotonically linked through the single structural parameter  $k$ . Across all tested networks and parameter combinations ( $\varphi \in [0.15, 0.28]$ ,  $\alpha = 0.10$ , BA/ER/WS topologies, and four real-world networks), we observe no Pareto improvement: uniform hub deletion worsens both metrics simultaneously in every case examined. We note that this is an empirical observation, not a proven impossibility result; whether alternative intervention classes—degree-preserving rewiring, weighted edge adjustment, or adaptive threshold modification—can decouple these functions is an important open question for future work.

This operational coupling is not merely definitional (“degree determines everything”). The non-trivial content is that real-world interventions operate on *nodes*, not on *functions*: reducing a bank’s counterparty connections to mitigate systemic risk necessarily reduces its capacity to absorb counterparty losses without propagating them. The coupling constrains the *feasible intervention space*, not just the mathematical description. This is analogous to pharmacological selectivity: a drug’s binding affinity to one receptor constrains its binding to structurally similar receptors, because the molecular recognition surface cannot be independently modified.

### B. Relation to Prior Work

**Watts (2002)** [47] described stable nodes conceptually, and Gleeson & Cahalane (2007) [51] derived the analytical cascade condition; we operationalize the stable-node mechanism as the quantitative condition  $k > 1/\varphi$  and isolate its dynamical nature through controlled experiments that vary hub thresholds independently of topology. The hub vulnerability experiment (§III) provides a direct experimental decomposition of the stable-node mechanism from connectivity effects in the context of cascade dynamics.

**Gleeson and Cahalane (2007) [51]** derived the cascade branching condition  $z_1 > 1$  for random networks. We extend this to the post-removal setting, deriving a closed-form  $z_1$  under the configuration-model approximation for targeted hub removal (§VC) and demonstrating that the  $z_1$  crossing explains the observed phase transition. Importantly, the cascade window expansion formula  $\varphi_{\text{post}}^*/\varphi_{\text{pre}}^* \approx 1/(1 - \rho)$  is not specific to the BA model: for *any* degree distribution,  $\rho$  measures the edge fraction incident to removed hubs, and the expansion factor  $1/(1 - \rho)$  follows from the configuration-model  $z_1$  framework. In homogeneous networks (Poisson, exponential),  $\rho \ll 1$  and the expansion is negligible; in heterogeneous networks (power-law, BA),  $\rho \sim 0.3\text{--}0.5$  and the expansion is substantial. The degree heterogeneity threshold  $\kappa > \sim 10$  is thus a proxy for  $\rho$  being large enough to produce an observable phase transition, not a fundamental constant of the BA model.

**Albert, Jeong and Barabási (2000) [49]** established the “robust yet fragile” duality for scale-free networks under percolation. We extend this to encompass threshold cascade dynamics, showing that the duality becomes *compounding vulnerability* under hub removal—both fragilities compound rather than trade off.

**Snyder and Cai (2022) [65]** study “degree-targeted cascades” on modular networks, but target which nodes to *seed* (initially activate), not which nodes to *remove*. The distinction is fundamental: seeding preserves the degree distribution while exploiting it; removal alters the degree distribution and shifts the cascade phase boundary itself. Our  $z_1$  derivation addresses the removal case, which requires the post-removal degree distribution  $P'(j)$  and operates in a different mathematical regime.

**Gleeson (2008) [64]** extended analytical cascade methods to correlated and modular networks in the static (unperturbed) case, providing the natural framework for extending our  $z_1$  derivation to networks with degree-degree correlations—a direction we identify as important future work. **Nishioka and Hasegawa (2022) [70]** extended the Watts model with differential thresholds based on proximity to initiators, and **Karimi and Holme (2021) [71]** extended it to temporal networks. Our work complements these by studying how *structural intervention* (hub removal) modifies cascade thresholds, a distinct mechanism from seed selection or temporal dynamics. **Lee et al. (2023) [73]** studied threshold cascades on signed networks, demonstrating that heterogeneous tie types can shift phase boundaries—analogueous to how hub removal shifts the cascade boundary in our setting.

**Morone and Makse (2015) [55]** and **Braunstein et al. (2016) [56]** optimize network dismantling for percolation fragmentation. Our results complement this literature by identifying the cascade side-effects of percolation-optimal interventions: dismantling strategies that efficiently fragment a network may simultaneously expand the cascade vulnerability window [66]. **Geng et al. (2021) [69]** proposed disassortative rewiring to

enhance robustness of scale-free networks against localized attack, and **Lv et al. (2022) [72]** modeled SF network response to multi-node removal with dynamical cascading failures—both addressing the same hub-vulnerability mechanism from the defense perspective. The interdependent network literature [74, 77] has identified dual failure pathways in *multi-layer* settings; our contribution shows that compounding vulnerability arises even in *single-layer* networks when two stress models operate on the same topology, through a mechanism that recent hybrid spinodal analyses [68, 75] may help classify.

### C. Real-World Network Validation

To validate beyond synthetic BA networks, we test on four real-world networks from Stanford SNAP with diverse degree distributions and clustering coefficients, applying the same hub removal protocol ( $\alpha = 0.10$ ) and cascade sweep ( $\varphi \in [0.05, 0.40]$ , 40 seeds per  $\varphi$ ). We estimate  $p_c$  using both the susceptibility-peak and  $S = 0.5$  methods.

TABLE VII. Real-world network validation of compounding vulnerability under hub removal ( $\alpha = 0.10$ ).  $\Delta F_p$ : percolation fragility change (susceptibility peak).  $C_{\text{max}}^{\text{pre/post}}$ : peak mean cascade size before/after hub removal across all  $\varphi$  values tested.

Network	$N$	$\kappa$	$C$	$\Delta F_p$	$C_{\text{max}}^{\text{pre}}$	$C_{\text{max}}^{\text{post}}$
p2p-Gnutella	6,299	17.7	0.011	+75%	< 0.01%	1.7%
Wiki-Vote	7,066	145.4	0.142	+594%	< 0.01%	6.0%
Bitcoin OTC <sup>†</sup>	5,881	72.0	–	+170% <sup>‡</sup>	0.06%	0.8%
CA-HepPh*	11,204	130.9	0.622	+58% <sup>‡</sup>	0.04%	2.9%

<sup>†</sup>Bitcoin OTC has  $\gamma < 2$ ; the finite- $\kappa$  analytical framework is not strictly applicable. <sup>‡</sup> $S = 0.5$  method used where susceptibility peak is unreliable. \*High clustering ( $C = 0.622$ ); susceptibility peak yields anomalous results.

Cascade amplification under hub removal occurs in all four networks. In absolute terms, post-removal cascade sizes range from  $\sim 0.8\text{--}6\%$  across the four networks at peak amplification (Table VII)—meaningful but not network-spanning. In all cases, hub removal shifts cascade activity from negligible ( $< 0.1\%$ ) to non-negligible (1–6%), confirming a transition from subcritical to non-trivial cascade regimes. The qualitative finding—that hub removal activates cascades at previously subcritical thresholds—is robust across all four networks and both percolation estimators.

Compounding vulnerability (both percolation and cascade worsening) is cleanly confirmed in p2p-Gnutella ( $\kappa = 17.7$ ,  $C = 0.011$ ;  $\Delta F_p = +75\%$  by susceptibility peak) and Wiki-Vote ( $\kappa = 145.4$ ,  $C = 0.142$ ;  $\Delta F_p = +594\%$ ). For Email-Enron ( $C = 0.497$ ) and CA-HepPh ( $C = 0.622$ ), the susceptibility-peak method gives anomalous percolation results ( $\Delta F_p = -6.8\%$  and

−80.4% respectively), while the  $S = 0.5$  method yields  $\Delta F_p = +31\%$  and  $+58\%$ . We report  $S = 0.5$  values for these two networks (marked ‡ in Table VII). This estimator disagreement arises in high-clustering networks where the susceptibility landscape has multiple peaks; it does not affect the cascade amplification, which is robust across all estimators and all four networks. However, we note that full compounding vulnerability is confirmed with a single estimator only for the two low-clustering networks.

More broadly, our BA-derived  $\kappa > \sim 10$  threshold predicts compounding vulnerability in real-world networks: yeast protein-protein interaction networks ( $\kappa \approx 17$  [62]), the World Wide Web ( $\kappa \approx 55$  [63]), and citation networks ( $\kappa > 100$ ). Conversely, power grids ( $\kappa \approx 2$ ) and regular-topology networks fall below the threshold.

#### D. Implications

**Financial regulation.** Breaking up systemically important financial institutions reduces individual institution size but may enable cascade defaults at stress levels that would be subcritical in the pre-breakup network, as large institutions also serve as loss-absorption barriers. The 2008 Lehman Brothers collapse illustrates: a hub failure in the interbank network ( $\kappa > 10$  for CDS counterparty networks [53, 59]) simultaneously fragmented lending connectivity and triggered cascade defaults—compounding vulnerability in practice.

**Infrastructure.** Achieving N-1 compliance through hub removal (decommissioning large substations) could expand the cascade vulnerability window. While power grids have low  $\kappa$  (mitigating the cascade phase transition), the 2003 Northeast Blackout demonstrates that high-load hub lines can trigger both fragmentation and cascading overloads when N-1 criteria are violated at hub nodes.

**Epidemic control.** Targeted vaccination of high-degree individuals is standard for SIR epidemics but removes nodes that block threshold-based behavioral cascades (vaccine hesitancy, misinformation adoption), potentially enabling cascades at previously subcritical thresholds. Social networks, with their heavy-tailed degree distributions ( $\kappa \gg 10$ ), are prime candidates for compounding vulnerability under targeted interventions.

#### E. Limitations

(i) We validate on synthetic networks with controlled degree heterogeneity and on multiple real-world networks from Stanford SNAP. The Bitcoin OTC Trust Network ( $N = 5,881$ ,  $\gamma \approx 1.9$ ) confirms the directional effect but, with  $\gamma < 2$  implying divergent  $\langle k^2 \rangle$ , the finite- $\kappa$  analytical framework of §V is not strictly applicable to this network; the agreement is empirical rather than analytical. (ii) The bond percolation threshold  $p_c$  is esti-

mated using the susceptibility peak method (maximum of the mean finite-cluster size), the standard approach in computational percolation [46]. We verify robustness by comparing against the  $S = 0.5$  crossing and the Molloy–Reed analytical estimate; all three methods confirm  $\Delta F_p \gg 0$  (Appendix A). (iii) We test sensitivity to threshold heterogeneity using Beta-distributed per-node thresholds centered on  $\varphi$  (Appendix D); the compounding vulnerability effect persists under moderate and high heterogeneity, with amplification ranging from  $+349\%$  to  $+1,955\%$  at  $\varphi = 0.22$ . (iv) The configuration-model approximation in §V C ignores BA disassortativity and the correlation structure induced by targeted removal. Appendix C validates the  $z_1$  framework on configuration-model networks (where it is exact by construction), confirming that the approximation captures the dominant mechanism and that BA-specific correlations partially *dampen* rather than create the effect. (v) Static networks are studied; adaptive rewiring could mitigate or amplify the effect. (vi) The Watts cascade model is one of several cascade mechanisms; generalization to load-redistribution [57], cascade-based attacks [60], and DebtRank [53] models is an important direction. (vii) The  $\kappa > \sim 10$  threshold is derived for BA networks; the precise threshold depends on both the degree distribution shape and the cascade threshold  $\varphi$ , and should be understood as a BA-specific onset condition rather than a distribution-independent constant.

## VII. CONCLUSION

We have demonstrated that in Barabási–Albert networks ( $N = 2,000$ ,  $m = 2$ ), hub removal can raise the bond percolation threshold from  $p_c = 0.174$  to  $0.776$  while simultaneously expanding the Watts cascade window, enabling global cascades at threshold values that were previously subcritical. The phase transition at  $\varphi = 0.22$ – $0.25$ —where mean cascade size jumps from  $< 1\%$  to  $\sim 23\%$  of the network (1,000 trials)—is the most striking consequence, and the vulnerability is *latent*: subcritical cascade behavior at these threshold values gives no warning of the system’s proximity to the phase boundary—a proximity that becomes critical only after hub removal shifts the system across it. In principle, a cascade-vulnerability diagnostic could detect this proximity, but in practice such diagnostics require knowledge of the post-intervention network, which is typically unavailable.

The hub vulnerability experiment establishes that cascade suppression is primarily dynamical (95% cascades from threshold modification alone vs. 19% from hub removal), and the  $z_1$  derivation provides an analytical expression for cascade window expansion under targeted hub removal, confirming the subcritical-to-supercritical crossing at  $\varphi = 0.22$  ( $z_1: 0.850 \rightarrow 1.195$ ). These results argue for multi-stress-model resilience assessment as standard practice: before applying any topological in-

tervention, evaluate its consequences under at least two fundamentally different failure dynamics.

## ACKNOWLEDGMENTS

The author thanks the open-source Python community for NetworkX and NumPy. Simulation code, random seeds, and data are publicly available for independent reproduction [76].

- 
- [1] S. Boccaletti, V. Latora, Y. Moreno, M. Chavez, and D.-U. Hwang, *Complex networks: Structure and dynamics*, Phys. Rep. **424**, 175 (2006).
- [2] J. Gao, B. Barzel, and A.-L. Barabási, *Universal resilience patterns in complex networks*, Nature **530**, 307 (2016).
- [3] A.-L. Barabási, *Network Science* (Cambridge University Press, Cambridge, 2016).
- [4] D. L. Alderson and J. C. Doyle, *Contrasting views of complexity and their implications for network-centric infrastructures*, IEEE Trans. Syst. Man Cybern. A **40**, 839 (2010).
- [5] D. Stauffer and A. Aharony, *Introduction to Percolation Theory* (CRC Press, Boca Raton, 2014).
- [6] M. E. J. Newman, *Networks: An Introduction* (Oxford University Press, Oxford, 2010).
- [7] M. E. J. Newman and R. M. Ziff, *Fast Monte Carlo algorithm for site or bond percolation*, Phys. Rev. E **64**, 016706 (2001).
- [8] D. J. Watts, *A simple model of global cascades on random networks*, Proc. Natl. Acad. Sci. U.S.A. **99**, 5766 (2002).
- [9] A.-L. Barabási and R. Albert, *Emergence of scaling in random networks*, Science **286**, 509 (1999).
- [10] R. Albert, H. Jeong, and A.-L. Barabási, *Error and attack tolerance of complex networks*, Nature **406**, 378 (2000).
- [11] R. Cohen, K. Erez, D. ben-Avraham, and S. Havlin, *Breakdown of the Internet under intentional attack*, Phys. Rev. Lett. **86**, 3682 (2001).
- [12] J. P. Gleeson and D. J. Cahalane, *Seed size strongly affects cascades on random networks*, Phys. Rev. E **75**, 056103 (2007).
- [13] P. S. Dodds and D. J. Watts, *Universal behavior in a generalized model of contagion*, Phys. Rev. Lett. **92**, 218701 (2004).
- [14] S. Battiston, M. Puliga, R. Kaushik, P. Tasca, and G. Caldarelli, *DebtRank: Too Central to Fail? Financial Networks, the FED and Systemic Risk*, Sci. Rep. **2**, 541 (2012).
- [15] D. S. Callaway, M. E. J. Newman, S. H. Strogatz, and D. J. Watts, *Network robustness and fragility: Percolation on random graphs*, Phys. Rev. Lett. **85**, 5468 (2000).
- [16] F. Morone and H. A. Makse, *Influence maximization in complex networks through optimal percolation*, Nature **524**, 65 (2015).
- [17] A. Braunstein, L. Dall’Asta, G. Semerjian, and L. Zdeborová, *Network dismantling*, Proc. Natl. Acad. Sci. U.S.A. **113**, 12368 (2016).
- [18] A. E. Motter, *Cascade control and defense in complex networks*, Phys. Rev. Lett. **93**, 098701 (2004).
- [19] M. Molloy and B. Reed, *A critical point for random graphs with a given degree sequence*, Random Struct. Algorithms **6**, 161 (1995).
- [20] A. G. Haldane and R. M. May, *Systemic risk in banking ecosystems*, Nature **469**, 351 (2011).
- [21] A. E. Motter and Y.-C. Lai, *Cascade-based attacks on complex networks*, Phys. Rev. E **66**, 065102 (2002).
- [22] D. J. Watts and S. H. Strogatz, *Collective dynamics of ‘small-world’ networks*, Nature **393**, 440 (1998).
- [23] H. Jeong, S. P. Mason, A.-L. Barabási, and Z. N. Oltvai, *Lethality and centrality in protein networks*, Nature **411**, 41 (2001).
- [24] R. Albert, H. Jeong, and A.-L. Barabási, *Diameter of the World-Wide Web*, Nature **401**, 130 (1999).
- [25] J. P. Gleeson, *Cascades on correlated and modular random networks*, Phys. Rev. E **77**, 046117 (2008).
- [26] D. Snyder and W. Cai, *Degree-targeted cascades on modular networks*, Phys. Rev. Res. **4**, 013040 (2022).
- [27] O. Artime, M. De Domenico, and A. Guilera, *Robustness and resilience of complex networks*, Nat. Rev. Phys. **6**, 114 (2024).
- [28] L. D. Valdez, L. M. Shekhtman, S. Havlin, and L. A. Braunstein, *Cascading failures in complex networks*, J. Complex Netw. **8**, cnaa013 (2020).
- [29] G. Pál, Z. Danku, A. Batool, D. Horváth, and F. Kun, *Scaling laws of failure dynamics on complex networks*, Sci. Rep. **13**, 19733 (2023).
- [30] H. Geng, Y. Xu, and W. Wang, *Global disassortative rewiring strategy for enhancing the robustness of scale-free networks against localized attack*, Phys. Rev. E **103**, 022313 (2021).
- [31] S. Nishioka and T. Hasegawa, *Cascading behavior of an extended Watts model on networks*, arXiv:2112.10524 [physics.soc-ph] (2022).
- [32] F. Karimi and P. Holme, *A temporal network version of Watts’s cascade model*, arXiv:2103.13604 [physics.soc-ph] (2021).
- [33] C. Lv et al., *Cascading failure in networks with dynamical behavior against multi-node perturbation*, Chaos Solitons Fractals **162**, 112397 (2022).
- [34] K. M. Lee et al., *Threshold cascade dynamics on signed random networks*, Chaos Solitons Fractals **168**, 113118 (2023).
- [35] W. Xu et al., *Breakdown in interdependent directed networks under targeted attacks*, Europhys. Lett. **133**, 68004 (2021).
- [36] I. Bonamassa, B. Gross, J. Kertész, and S. Havlin, *Hybrid spinodals for long-range cascades*, arXiv:2401.09313 [cond-mat.stat-mech] (2024).
- [37] F. Cachero, *Cascade Window Paradox: simulation code, data, and Lean 4 proofs*, <https://github.com/Freddy-Cach/cascade-window-paradox> (2026).
- [38] C. D. Brummitt, R. M. D’Souza, and E. A. Leicht, *Suppressing cascades of load in interdependent networks*, Proc. Natl. Acad. Sci. U.S.A. **109**, E680 (2012).
- [39] R. Cohen, K. Erez, D. ben-Avraham, and S. Havlin, *Re-*

- silience of the Internet to random breakdowns*, Phys. Rev. Lett. **85**, 4626 (2000).
- [40] S. Boccaletti, V. Latora, Y. Moreno, M. Chavez, and D.-U. Hwang, *Complex networks: Structure and dynamics*, Phys. Rep. **424**, 175 (2006).
- [41] J. Gao, B. Barzel, and A.-L. Barabási, *Universal resilience patterns in complex networks*, Nature **530**, 307 (2016).
- [42] A.-L. Barabási, *Network Science* (Cambridge University Press, Cambridge, 2016).
- [43] D. L. Alderson and J. C. Doyle, *Contrasting views of complexity and their implications for network-centric infrastructures*, IEEE Trans. Syst. Man Cybern. A **40**, 839 (2010).
- [44] D. Stauffer and A. Aharony, *Introduction to Percolation Theory* (CRC Press, Boca Raton, 2014).
- [45] M. E. J. Newman, *Networks: An Introduction* (Oxford University Press, Oxford, 2010).
- [46] M. E. J. Newman and R. M. Ziff, *Fast Monte Carlo algorithm for site or bond percolation*, Phys. Rev. E **64**, 016706 (2001).
- [47] D. J. Watts, *A simple model of global cascades on random networks*, Proc. Natl. Acad. Sci. U.S.A. **99**, 5766 (2002).
- [48] A.-L. Barabási and R. Albert, *Emergence of scaling in random networks*, Science **286**, 509 (1999).
- [49] R. Albert, H. Jeong, and A.-L. Barabási, *Error and attack tolerance of complex networks*, Nature **406**, 378 (2000).
- [50] R. Cohen, K. Erez, D. ben-Avraham, and S. Havlin, *Breakdown of the Internet under intentional attack*, Phys. Rev. Lett. **86**, 3682 (2001).
- [51] J. P. Gleeson and D. J. Cahalane, *Seed size strongly affects cascades on random networks*, Phys. Rev. E **75**, 056103 (2007).
- [52] P. S. Dodds and D. J. Watts, *Universal behavior in a generalized model of contagion*, Phys. Rev. Lett. **92**, 218701 (2004).
- [53] S. Battiston, M. Puliga, R. Kaushik, P. Tasca, and G. Caldarelli, *DebtRank: Too Central to Fail? Financial Networks, the FED and Systemic Risk*, Sci. Rep. **2**, 541 (2012).
- [54] D. S. Callaway, M. E. J. Newman, S. H. Strogatz, and D. J. Watts, *Network robustness and fragility: Percolation on random graphs*, Phys. Rev. Lett. **85**, 5468 (2000).
- [55] F. Morone and H. A. Makse, *Influence maximization in complex networks through optimal percolation*, Nature **524**, 65 (2015).
- [56] A. Braunstein, L. Dall’Asta, G. Semerjian, and L. Zdeborová, *Network dismantling*, Proc. Natl. Acad. Sci. U.S.A. **113**, 12368 (2016).
- [57] A. E. Motter, *Cascade control and defense in complex networks*, Phys. Rev. Lett. **93**, 098701 (2004).
- [58] M. Molloy and B. Reed, *A critical point for random graphs with a given degree sequence*, Random Struct. Algorithms **6**, 161 (1995).
- [59] A. G. Haldane and R. M. May, *Systemic risk in banking ecosystems*, Nature **469**, 351 (2011).
- [60] A. E. Motter and Y.-C. Lai, *Cascade-based attacks on complex networks*, Phys. Rev. E **66**, 065102 (2002).
- [61] D. J. Watts and S. H. Strogatz, *Collective dynamics of ‘small-world’ networks*, Nature **393**, 440 (1998).
- [62] H. Jeong, S. P. Mason, A.-L. Barabási, and Z. N. Oltvai, *Lethality and centrality in protein networks*, Nature **411**, 41 (2001).
- [63] R. Albert, H. Jeong, and A.-L. Barabási, *Diameter of the World-Wide Web*, Nature **401**, 130 (1999).
- [64] J. P. Gleeson, *Cascades on correlated and modular random networks*, Phys. Rev. E **77**, 046117 (2008).
- [65] D. Snyder and W. Cai, *Degree-targeted cascades on modular networks*, Phys. Rev. Res. **4**, 013040 (2022).
- [66] O. Artime, M. De Domenico, and A. Guilera, *Robustness and resilience of complex networks*, Nat. Rev. Phys. **6**, 114 (2024).
- [67] L. D. Valdez, L. M. Shekhtman, S. Havlin, and L. A. Braunstein, *Cascading failures in complex networks*, J. Complex Netw. **8**, cnaa013 (2020).
- [68] G. Pál, Z. Danku, A. Batool, D. Horváth, and F. Kun, *Scaling laws of failure dynamics on complex networks*, Sci. Rep. **13**, 19733 (2023).
- [69] H. Geng, Y. Xu, and W. Wang, *Global disassortative rewiring strategy for enhancing the robustness of scale-free networks against localized attack*, Phys. Rev. E **103**, 022313 (2021).
- [70] S. Nishioka and T. Hasegawa, *Cascading behavior of an extended Watts model on networks*, arXiv:2112.10524 [physics.soc-ph] (2022).
- [71] F. Karimi and P. Holme, *A temporal network version of Watts’s cascade model*, arXiv:2103.13604 [physics.soc-ph] (2021).
- [72] C. Lv *et al.*, *Cascading failure in networks with dynamical behavior against multi-node perturbation*, Chaos Solitons Fractals **162**, 112397 (2022).
- [73] K. M. Lee *et al.*, *Threshold cascade dynamics on signed random networks*, Chaos Solitons Fractals **168**, 113118 (2023).
- [74] W. Xu *et al.*, *Breakdown in interdependent directed networks under targeted attacks*, Europhys. Lett. **133**, 68004 (2021).
- [75] I. Bonamassa, B. Gross, J. Kertész, and S. Havlin, *Hybrid spinodals for long-range cascades*, arXiv:2401.09313 [cond-mat.stat-mech] (2024).
- [76] F. Cachero, *Cascade Window Paradox: simulation code, data, and Lean 4 proofs*, <https://github.com/Freddy-Cach/cascade-window-paradox> (2026).
- [77] C. D. Brummitt, R. M. D’Souza, and E. A. Leicht, *Suppressing cascades of load in interdependent networks*, Proc. Natl. Acad. Sci. U.S.A. **109**, E680 (2012).
- [78] R. Cohen, K. Erez, D. ben-Avraham, and S. Havlin, *Resilience of the Internet to random breakdowns*, Phys. Rev. Lett. **85**, 4626 (2000).

## Appendix A: Percolation Method Comparison

TABLE VIII. Comparison of  $p_c$  estimates across methods. “Susc. peak” is the susceptibility maximum (primary, Sec. II), “ $S = 0.5$ ” is the giant component crossing, and “MR” is the Molloy–Reed analytical estimate.

Network	$p_c$ (susc.)	$p_c$ ( $S = 0.5$ )	$p_c$ (MR)	$\Delta F_p$ (susc.)
BA before	0.174	0.337	0.092	—
BA after	0.776	0.903	0.240	+347%
ER before	—	0.354	0.251	—
WS before	—	0.499	0.323	—

The  $\sim 3.5\times$  discrepancy for BA networks reflects disassortativity and finite-size effects absent from the Molloy-Reed configuration-model assumption. The qualitative result (massive  $\Delta F_p$  increase) is robust to method choice.

### Appendix B: $z_1$ Derivation Details

The BA degree distribution is  $P(k) = 2m(m+1)/[k(k+1)(k+2)]$  for  $k \geq m$ . The edge-to-hub probability  $\rho = (m+1)/(k_{\text{cut}}+2)$  follows from the excess degree distribution. The post-removal  $z_1$  involves summing  $j(j-1)P'(j)/\langle k \rangle'$  over vulnerable nodes  $j \leq \lfloor 1/\varphi \rfloor$ , where  $P'(j)$  is the binomial convolution of  $P(k)$  with edge retention probability  $(1-\rho)$ . Under the mean-field approximation, this yields the closed-form harmonic-number expression in §VC, with partial fractions:  $(k-1)/[(k+1)(k+2)] = -2/(k+1) + 3/(k+2)$ . Python verification code and scripts are available at <https://github.com/Freddy-Cach/cascade-window-paradox>.

### Appendix C: Configuration-Model Validation

To validate the  $z_1$  derivation (§VC), which assumes configuration-model independence, we test on configuration-model networks constructed with the same degree sequence as BA ( $N = 2,000$ ,  $m = 2$ ). For each of 20 BA realizations, we generate a matched configuration-model network (removing self-loops and multi-edges), apply the same hub removal protocol, and compare cascade behavior.

TABLE IX. Configuration-model validation ( $N = 2,000$ ,  $m = 2$ ,  $\varphi = 0.22$ , 20 networks  $\times$  20 seeds). The configuration model shows *stronger* cascades than BA, confirming that BA-specific degree correlations partially suppress the effect.

Network	$\kappa$	$p_c^{\text{pre}}$	$p_c^{\text{post}}$	Post cascade
BA	$12.0 \pm 0.6$	0.181	0.788	22.9%
Config model	$11.4 \pm 0.5$	0.159	0.751	38.1%

The configuration-model networks exhibit *stronger* cascade amplification (38.1% vs 22.9%) and similar percolation degradation. This confirms two claims: (i) the  $z_1$  framework accurately predicts cascade window expansion for configuration-model networks, where it is exact by construction; (ii) BA disassortativity partially *dampens* the cascade effect—high-degree hubs preferentially connect to low-degree stubs, creating extra “firewall” correlations absent in uncorrelated networks. The analyti-

cal upper-bound character of Eq. 3 is thus validated: the true BA cascade size lies below the configuration-model prediction.

### Appendix D: Heterogeneous Threshold Sensitivity

To test whether compounding vulnerability depends on the assumption of uniform thresholds, we replace the fixed  $\varphi = 0.22$  with per-node thresholds drawn from three distributions, each centered on  $\varphi = 0.22$ : (i) Uniform(0.12, 0.32), (ii) Beta with low heterogeneity ( $\alpha = 5, \beta = 17.7, \sigma \approx 0.08$ ), and (iii) Beta with high heterogeneity ( $\alpha = 2, \beta = 7.1, \sigma \approx 0.13$ ). Each condition uses 600 trials (15 networks  $\times$  40 seeds).

TABLE X. Heterogeneous threshold sensitivity ( $\varphi = 0.22$ , 600 trials each). “Amp.” is the amplification at  $\varphi = 0.22$ ; the maximum across all  $\varphi$  (peaking at  $\varphi \approx 0.24$ ) is larger in all cases.

Distribution	Pre (%)	Post (%)	Amp.
Uniform (homogeneous)	1.0	21.6	+1,955%
Beta (low het.)	1.3	25.1	+1,830%
Beta (high het.)	4.0	18.0	+349%

Under all three distributions, hub removal produces massive cascade amplification at the transition (+349% to +1,955% at  $\varphi = 0.22$ ; amplification peaks at  $\varphi \approx 0.24$  in all cases). High heterogeneity reduces the effect because some nodes have thresholds well below 0.22, making them vulnerable even when hubs are present—partially pre-empting the firewall destruction mechanism. Critically, the *qualitative* effect (subcritical  $\rightarrow$  supercritical transition) persists: compounding vulnerability is not an artifact of uniform thresholds.

### Appendix E: Simulation Code and Formal Proofs

All simulation code, figure-generation scripts, and derived datasets are available at <https://github.com/Freddy-Cach/cascade-window-paradox>.

A Lean 4 formalization of key analytical claims from §V is provided in `proofs/` in the same repository, including the stable-node condition (Definition 1), the cascade onset bound (Observation 1), and the monotonicity of  $p_c$  under hub removal (Proposition 1). These machine-verified proofs establish the mathematical correctness of the cascade-blocking inequalities independently of the simulation results.

Key scripts: `simulate_production.py` (finite-size scaling), `phi_sweep_large.py` ( $\varphi$ -sweep), `hub_vulnerability_test.py` (§III experiment), `heterogeneous_threshold_test.py` (Appendix D).